

# Geophysical Research Letters

## RESEARCH LETTER

10.1029/2018GL080696

### Key Points:

- MMS observations reveal KSMDs coupled with whistler mode waves, electrostatic solitary waves, and electron cyclotron waves
- These waves are excited by different plasma distributions, and the ESWs could affect the electron distributions in kinetic scale
- Statistical results indicate that the KSMDs in the magnetosheath are a possible origin for various kinds of waves

### Supporting Information:

- Supporting Information S1

### Correspondence to:

Q. Q. Shi,  
sqq@pku.edu.cn

### Citation:

Yao, S. T., Shi, Q. Q., Yao, Z. H., Li, J. X., Yue, C., Tao, X., et al. (2019). Waves in kinetic-scale magnetic dips: MMS observations in the magnetosheath. *Geophysical Research Letters*, 46, 523–533. <https://doi.org/10.1029/2018GL080696>

Received 29 SEP 2018

Accepted 12 DEC 2018

Accepted article online 17 DEC 2018

Published online 16 JAN 2019

## Waves in Kinetic-Scale Magnetic Dips: MMS Observations in the Magnetosheath

S. T. Yao<sup>1,2</sup> , Q. Q. Shi<sup>1</sup> , Z. H. Yao<sup>3,4</sup> , J. X. Li<sup>5</sup>, C. Yue<sup>5</sup> , X. Tao<sup>6</sup> , A. W. Degeling<sup>1</sup> , Q. G. Zong<sup>7</sup> , X. G. Wang<sup>8</sup> , A. M. Tian<sup>1</sup> , C. T. Russell<sup>9</sup> , X. Z. Zhou<sup>7</sup> , R. L. Guo<sup>10</sup> , I. J. Rae<sup>3</sup> , H. S. Fu<sup>11</sup> , H. Zhang<sup>12</sup> , L. Li<sup>8</sup> , O. Le Contel<sup>13</sup> , R. B. Torbert<sup>14</sup> , R. E. Ergun<sup>15</sup> , P.-A. Lindqvist<sup>16</sup> , C. J. Pollock<sup>17</sup> , and B. L. Giles<sup>17</sup> 

<sup>1</sup>Shandong Provincial Key Laboratory of Optical Astronomy and Solar-Terrestrial Environment, Institute of Space Sciences, Shandong University, Weihai, China, <sup>2</sup>State Key Laboratory of Space Weather, National Space Science Center, Chinese Academy of Sciences, Beijing, China, <sup>3</sup>Mullard Space Science Laboratory, University College London, London, UK, <sup>4</sup>Laboratoire de Physique Atmosphérique et Planétaire, STAR Institute, Université de Liège, Liège, Belgium,

<sup>5</sup>Department of Atmospheric and Oceanic Sciences, University of California, Los Angeles, CA, USA, <sup>6</sup>CAS Key Laboratory of Geospace Environment, Department of Geophysics and Planetary Sciences, University of Science and Technology of China, Hefei, China, <sup>7</sup>School of Earth and Space Sciences, Peking University, Beijing, China, <sup>8</sup>Department of Physics, Harbin Institute of Technology, Harbin, China, <sup>9</sup>Department of Earth, Planetary and Space Sciences, University of California, Los Angeles, CA, USA, <sup>10</sup>Key Laboratory of Earth and Planetary Physics, Institute of Geology and Geophysics, Chinese Academy of Sciences, Beijing, China, <sup>11</sup>School of Space and Environment, Beihang University, Beijing, China, <sup>12</sup>Physics Department and Geophysical Institute, University of Alaska Fairbanks, Fairbanks, AK, USA, <sup>13</sup>Laboratoire de Physique des Plasmas, UMR7648, CNRS, Ecole Polytechnique, Sorbonne Universités, Université Paris-Sud, Observatoire de Paris, Paris, France, <sup>14</sup>Department of Physics, University of New Hampshire, Durham, NH, USA, <sup>15</sup>Department of Astrophysical and Planetary Sciences, University of Colorado Boulder, Boulder, CO, USA, <sup>16</sup>Royal Institute of Technology, Stockholm, Sweden, <sup>17</sup>NASA Goddard Space Flight Center, Greenbelt, MD, USA

**Abstract** Kinetic-scale magnetic dips (KSMDs), with a significant depression in magnetic field strength, and scale length close to and less than one proton gyroradius, were reported in the turbulent plasmas both in recent observation and numerical simulation studies. These KSMDs likely play important roles in energy conversion and dissipation. In this study, we present observations of the KSMDs that are labeled whistler mode waves, electrostatic solitary waves, and electron cyclotron waves in the magnetosheath. The observations suggest that electron temperature anisotropy or beams within KSMD structures provide free energy to generate these waves. In addition, the occurrence rates of the waves are higher in the center of the magnetic dips than at their edges, implying that the KSMDs might be the origin of various kinds of waves. We suggest that the KSMDs could provide favorable conditions for the generation of waves and transfer energy to the waves in turbulent magnetosheath plasmas.

**Plain Language Summary** The Earth's magnetosheath is a turbulent plasma environment where energy conversion, particle acceleration, and mass and momentum transport take place. Many of these key processes involve kinetic-scale physics. However, in-depth studies from previous missions are limited by their lower spacecraft data resolution. The recent Magnetospheric Multiscale (MMS) mission provides us with a large amount of high-temporal cadence data for studying kinetic-scale physics in the magnetosheath. In this study, we report whistler mode waves, electrostatic solitary waves and electron cyclotron waves within kinetic-scale magnetic dips (KSMDs) that can be generated in the turbulent magnetosheath. These waves could be excited by electron temperature anisotropy or beams. As is well known, plasma waves are important processes in converting energy, accelerating and scattering electrons and ions, and modifying the distributions of charged particles. If plasma instabilities develop within the KSMDs, the resulting waves could absorb free energy from plasma particles and may propagate out of the KSMDs. Thus, our discoveries could significantly advance the understanding of energy conversion and dissipation for kinetic-scale turbulence. This study provides a new reference not only for observations in space physics but also for related basic plasma theories and numerical simulations.

## 1. Introduction

Kinetic-scale magnetic dips (KSMDs) are a significant depression of magnetic field strength with a scale size close to or less than a proton gyroradius ( $\rho_i$ ). These structures have been observed both in the Earth's magnetospheric plasma sheet (e.g., Ge et al., 2011; Gershman et al., 2016; Goodrich et al., 2016; Sun et al., 2012; Sundberg et al., 2015; Yao et al., 2016; Zhima et al., 2015; Zhang et al., 2017) and magnetosheath (e.g., Huang, Sahraoui, et al., 2017; Yao et al., 2017). In addition to observational investigations, KSMDs have also been extensively studied through theoretical analysis and numerical simulations (e.g., Balikhin et al., 2012; Haynes et al., 2015; Ji et al., 2014; Li et al., 2016; Roytershteyn et al., 2015). The KSMD structures have similar observational characteristics to the magnetic mirror mode (MM; Tsurutani et al., 1982; Yao, Shi, Liu, et al., 2018), magnetic hole (MH), and interplanetary magnetic decreases (MD; Shi et al., 2009; Tsurutani et al., 1994, 1999; Tsurutani, Dasgupta, et al., 2002; Tsurutani et al., 2009; Xiao et al., 2010, 2014) reported in previous studies; however, their formation processes and relevant physics are distinct. The classifications, generation mechanisms, and related studies (e.g., proton cyclotron and Langmuir waves inside the MD) for the MM, MH, and MD are well discussed by Tsurutani et al. (2011) and related works (Lin et al., 1996; Tsurutani, Galvan, et al., 2002; Tsurutani, Dasgupta, et al., 2002; Tsurutani et al., 2005, 2018).

The magnetosheath is a turbulent plasma environment where energy conversion, particle acceleration, and mass and momentum transport take place. Many of these key processes involve kinetic-scale physics. With measurements of high-temporal cadence from the Magnetospheric Multiscale (MMS) mission (Burch et al., 2016), the KSMDs and some possible related structures were reported in the turbulent magnetosheath (Huang, Sahraoui, et al., 2017; Yao et al., 2017; Yao, Shi, Guo, et al., 2018) and are thought to play an important role in dissipating energy (Huang, Sahraoui, et al., 2017). In addition, from recent two- and three-dimensional particle-in-cell simulations, the KSMDs were found in turbulent magnetized plasmas (Haynes et al., 2015; Roytershteyn et al., 2015). Though KSMDs in turbulent plasmas have been studied both by observations and simulations, whether there is energy dissipation or conversion in KSMDs, and how this occurs are not yet understood.

Plasma waves are important processes in converting energy, accelerating and scattering charged particles, and modifying the distributions of ions and electrons (e.g., Li, Zhou, Zong, Chen, et al., 2017; Li, Zhou, Zong, Rankin, et al., 2017; Lin et al., 1996; Shi et al., 2013, 2014; Sun et al., 2015; Thorne et al., 2006, 2010; Tsurutani, Galvan, et al., 2002; Zhang et al., 2010; Zong et al., 2007). If plasma instabilities develop within the KSMDs, waves could be locally generated in KSMDs and absorb free energy from plasma and may propagate out of the KSMDs. In addition, waves can be used as a tool to infer microscale particle dynamics, which could significantly advance our understanding of the KSMD dynamics.

Whistler mode electromagnetic waves have been observed in magnetic depressions in the terrestrial magnetosheath for more than 40 years. They are known as *lion roars* with central frequencies  $\sim$ 100 Hz, and the magnetic depressions are termed as *mirror mode* (e.g., Smith et al., 1969; Smith & Tsurutani, 1976; Tsurutani et al., 1982). It should be noted that the mirror mode is not a kinetic-scale structure (Tsurutani et al., 2011). Here we just giving an example of similar waves detected in larger-scale structures. Over the past decades, a majority of works focused on lion roars associated with magnetohydrodynamic-scale magnetic depressions. However, these waves were seldom observed in KSMDs due to the low time resolution of available observations. Electrostatic solitary waves (ESWs) are characterized by solitary or continuous bipolar electric field pulses parallel to the background magnetic field (Lakhina et al., 2000; Matsumoto et al., 1997). They were first observed in the plasma sheet boundary layer as a component of broadband electrostatic noise (Matsumoto et al., 1994, 1997) and were widely observed in space plasmas, such as in the solar wind (Mangeney et al., 1999), the distant magnetosheath (Kojima et al., 1997), the plasma sheet boundary (Cattell et al., 1999), the Earth's bow shock (Bale et al., 1998; Matsumoto et al., 1997), the magnetopause (Matsumoto et al., 2000; Mozer et al., 1997), and the magnetotail (Andersson et al., 2009; Le Contel et al., 2017; Tao et al., 2011). Their spatial sizes are on the order of several Debye lengths and could be generated from the two-stream instability (e.g., Goldman et al., 1999). A possible generation mechanism is that the parallel electric field component of two obliquely propagating proton cyclotron waves accelerate electrons toward each other, providing free energy for the generation of the ESWs (Tsurutani et al., 2003). Because of the ESW's nonlinear generation process, they are termed as *electron phase-space density holes*, and they

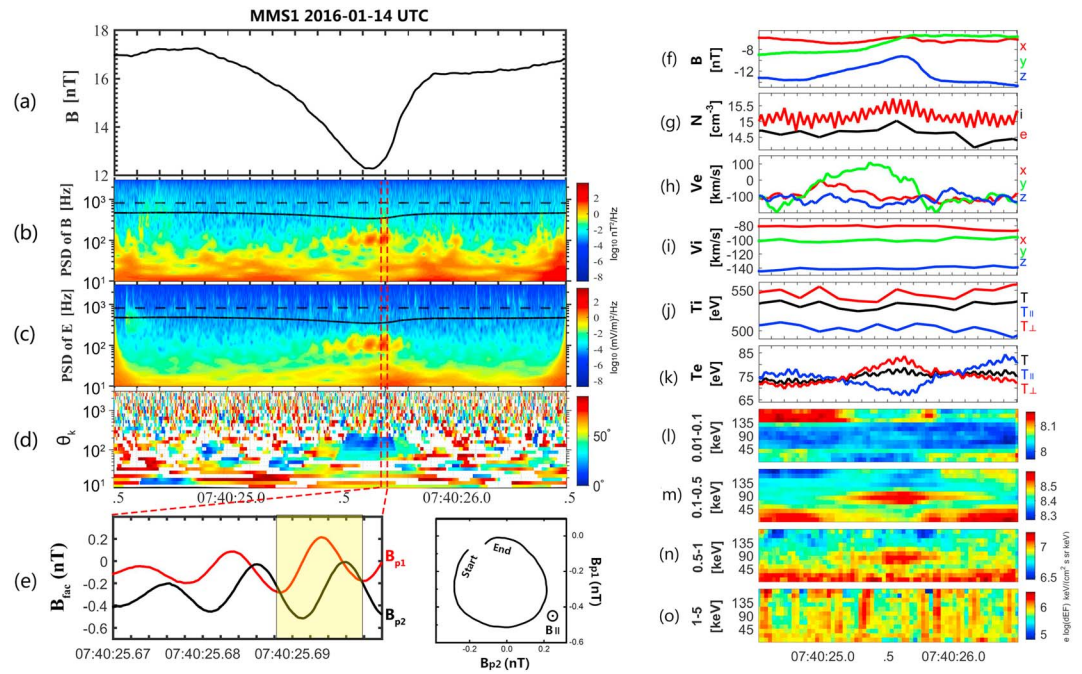


**Figure 1.** Whistler mode waves (WHs) observed in the kinetic-scale magnetic dips (KSMDs). (a) Total magnetic field strength. (b and c) Power spectral densities (PSDs) of the electric and magnetic fields overplotted with the electron cyclotron frequency (solid line) and ion plasma frequency (dashed line). (d) Wave normal angle. (e) Magnetic field in field-aligned coordinates and their hodograph during a short interval marked by the two vertical dashed lines in the above panels. The  $B_{p1}$  and  $B_{p2}$  are the magnetic field of two perpendicular directions. (f) Magnetic field components. (g) Ion and electron number densities. (h and i) Ion and electron velocity components. (j and k) Ion and electron temperatures. Plasma properties in (g)–(k) are calculated by taking the moments from the 3-D particle distributions from 10 eV to 30 keV. (l–o) Electron pitch angle distributions.

can be modeled using the Bernstein-Greene-Kruskal modes (e.g., Chen & Parks, 2002a, 2002b; Muschietti, et al., 1999). Another interpretation for ESWs observed in space plasmas is that these structures could be ion- and electron-acoustic solitons (e.g., Lakhina et al., 2018; Rubia et al., 2017).

In this study, we report new discoveries of various kinds of electromagnetic and electrostatic waves within the dayside magnetosheath KSMDs. These waves include whistler mode waves (WHs), ESWs, and electron cyclotron waves (ECWs). The source and generation mechanisms of these waves, and their effects and importance are discussed. The data and event selection criterion are shown in the supporting information.

## 2. Observations

### 2.1. Observations of Electromagnetic Waves

Figure 1 shows an example associated with WH activity observed by MMS1 at  $[9.2, -4.0, -0.9]$   $R_E$  (Earth radii). The total magnetic field strength shown in Figure 1a decreases significantly from 16.6 to 12.3 nT in  $\sim 1$  s. The scale of the KSMD is  $\sim 1.4 \rho_i$  ( $\rho_i \sim 140$  km, calculated from the background magnetic field  $B = 16.6$  nT and ion energy  $E = 540$  eV), obtained from the averaged background ion bulk velocity ( $V \sim 190$  km/s) and the duration ( $\Delta t \sim 1$  s), assuming that the structure is convected by the magnetosheath flow. Figures 1b and 1c display the power spectral densities of the magnetic and electric fields related to the KSMD. Strong magnetic and electric wave powers at  $\sim 100$  Hz are found in the center of the KSMD. Their central frequency  $f$  is  $\sim 0.25 f_{ce}$  (the local electron cyclotron frequency, black solid line) and is much lower than  $f_{pi}$  (the ion plasma frequency, black dashed line). The wave normal angle ( $\theta_k$ ) is  $\sim 15^\circ$ , nearly parallel to the ambient magnetic field (Figure 1d, obtained from the singular value decomposition method; Santoli'k et al., 2003). The waves are right-handed circularly polarized, as can be seen from the perpendicular magnetic field variation during the time interval indicated by the yellow shaded region in Figure 1e. These wave characteristics indicate that the waves are electromagnetic WHs. By estimating  $|\Delta E_{\perp p1}/\Delta B_{\perp p1}|$ , where

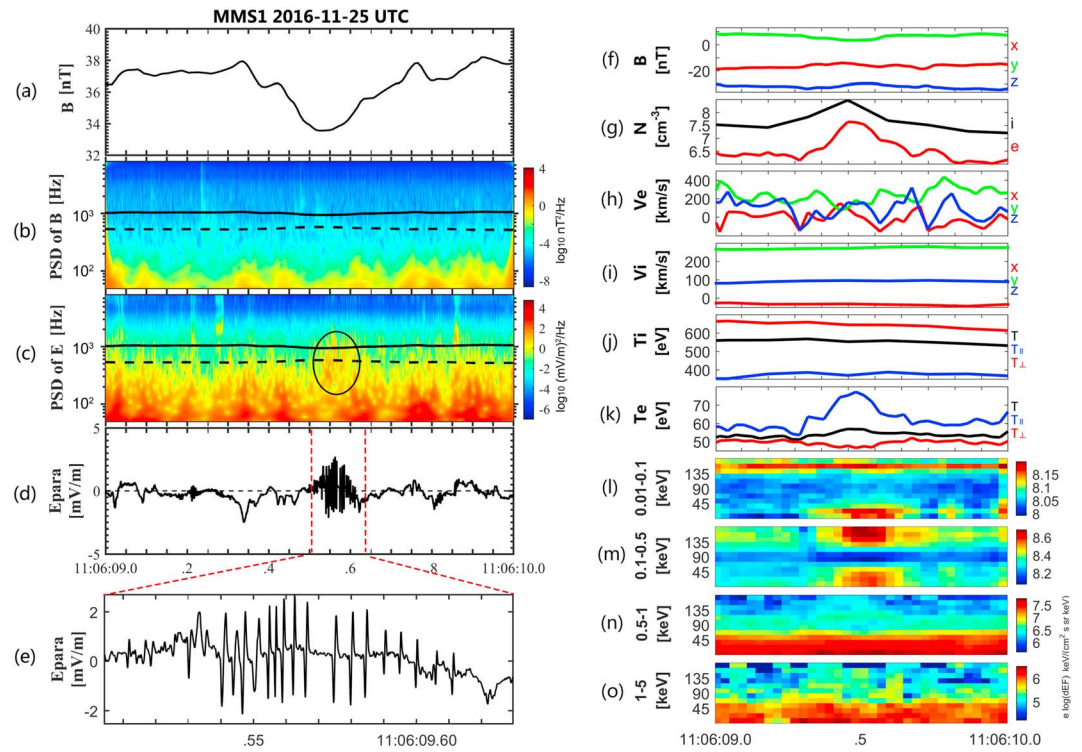


**Figure 2.** Electrostatic solitary waves (ESWs) observed in the KSMDs. (a–c) and (f–o) same as Figure 1. (d and e) Parallel electric field and an expanded view of the parallel electric field during a selected period. Plasma properties in (g–k) are calculated by taking the moments from the 3-D particle distributions from 10 eV to 30 keV.

$\Delta E_{\perp p1}$  and  $\Delta B_{\perp p2}$  are the perpendicular wave electric and magnetic fields, we found that the phase speed of the wave ( $v_{ph}$ ) is  $\sim 2,500$  km/s.

In Figure 1, the depression of the magnetic field in the KSMD is mainly due to the change in the z component (Figure 1f, blue line); variations of plasma density are not obvious for both ions and electrons (Figure 1g). The ion and electron number densities given here are not the total densities but measured over a limited energy range. This results in an apparent inequality in ion and electron number densities reported in this study, see details in the supporting information. In addition, the ion temperatures do not change significantly across the KSMD, whereas the electron temperature anisotropy  $T_{e\perp}/T_{e\parallel}$  develops a value substantially greater than unity in the same interval, as shown in Figure 1k. It is shown that electron fluxes increase near  $90^\circ$  from 0.1 to 1 keV (Figures 1l and 1m), which leads to the temperature anisotropy. According to the cyclotron resonance condition (e.g., Cao et al., 2017; Fu et al., 2012; Kennel & Engelmann, 1966; Wilson et al., 2013), the minimum resonant electron energy is of 130–160 eV. Anisotropic electron distributions are observed in Figures 1l and 1m over the energy range of 100–1,000 eV, suggesting that the WHs could possibly be generated by these anisotropic electron populations (e.g., Gary & Karimabadi, 2006; Huang et al., 2012; Fu et al., 2011; Li, Bortnik, et al., 2017).

## 2.2. Observations of Electrostatic Waves

Figure 2 shows an overview of a KSMD event associated with ESWs observed at  $[10.3, 5.7, 0.2] R_E$  by MMS1. The total magnetic field strength, displayed in Figure 2a, shows a rapid decrease from  $\sim 38$  to  $\sim 33$  nT in 0.4 s. The scale of the KSMD is  $\sim 1.9 \rho_i$ , obtained from  $V \sim 300$  km/s (assuming nonpropagating structure in the magnetosheath flow) and  $\Delta t \sim 0.4$  s, and  $\rho_i \sim 62$  km from  $B = 38$  nT and  $E = 550$  eV. Given that there were no significant corresponding magnetic fluctuations (Figure 2bc), the waves appear to be electrostatic and their frequencies are close to  $f_{ce}$  and  $f_{pi}$ . Significant bi-polar structures in the parallel wave electric field can be in Figure 2e. These features are observed by all four MMS spacecraft, and we thus use the timing method (Paschmann et al., 1998; Russell et al., 1983) to determine their propagation velocities. The results

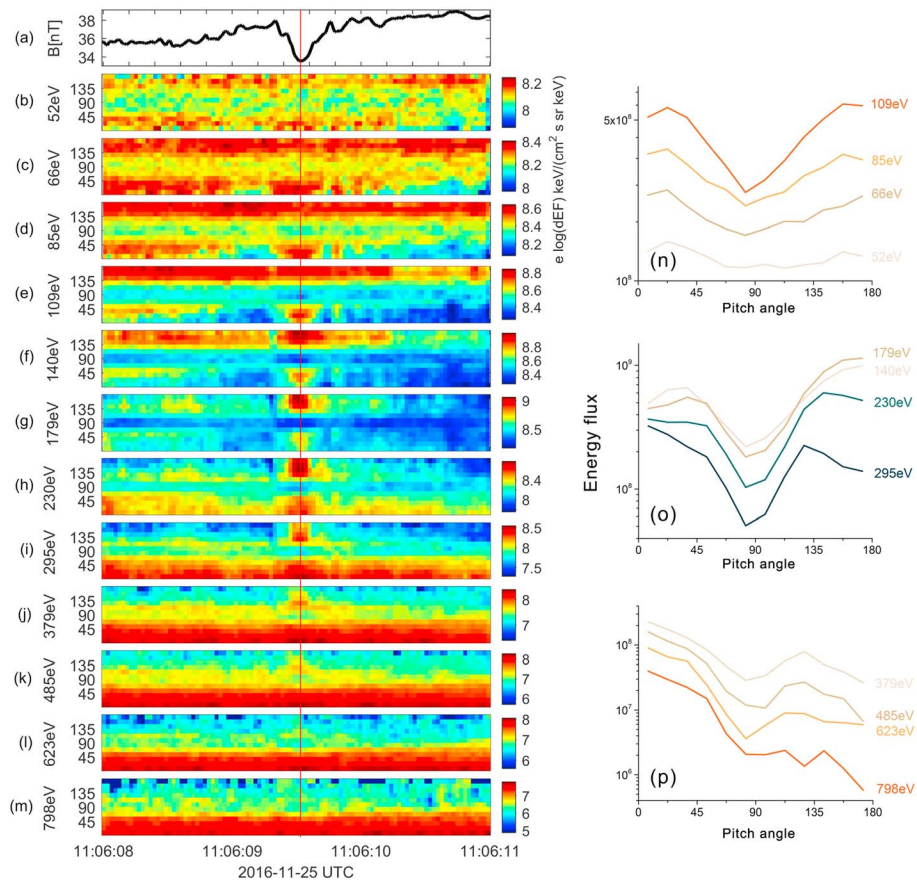


**Figure 3.** (a) Total magnetic field strength. (b–m) Electron pitch angle distributions. (n–p) Energy fluxes versus pitch angle, at the time marked by the red vertical line in (a)–(m).

range from 4350 km/s to 4970 km/s. This corresponds to a resonant electron energy of several tens eV. The densities of both ions and electrons are enhanced within the KSMD (Figure 2g). The ion bulk velocity and temperatures do not change significantly across the KSMD (Figures 2i–2j), but the electron temperature anisotropy decreases from  $T_{e\perp}/T_{e\parallel} \approx 0.86$  outside to  $T_{e\perp}/T_{e\parallel} \approx 0.61$  inside the structure. From the electron PADs measured by MMS1, we find that the electron energy fluxes mainly rose near  $0^\circ$  and  $180^\circ$  pitch angles from 0.1 keV to 0.5 keV (Figure 2m), suggesting that the ESWs may be generated by the electron two-stream instability (e.g., Chen et al., 2003; Goldman et al., 1999).

Figure 3 displays the details of the electron PADs. The parallel and antiparallel energy fluxes increased significantly from  $\sim 80$  eV to  $\sim 300$  eV inside the KSMD, and the perpendicular energy fluxes were always lower than that of the other angles (Figures 3b–3l). It is clear that the energy fluxes near  $90^\circ$  from  $\sim 80$  eV to  $\sim 700$  eV were lower than that of the other pitch angles from Figures 3a–3m. In previous studies, Yao et al. (2017) found KSMDs in the magnetosheath with perpendicular energy fluxes increasing from  $\sim 80$  eV to  $\sim 800$  eV. Similar features were reported in the Earth's plasma sheet by Sun et al., 2012 and Gershman et al. (2016) and in the magnetosheath by Huang, Sahraoui, et al. (2017). In a recent statistical study, Huang, Du, et al. (2017) showed that the electron fluxes at 71–850 eV were significantly enhanced at  $\sim 90^\circ$  pitch angles for most events in the magnetosheath. However, these observed features are opposite to our finding. It should be noted that, although the increase of the energy fluxes in parallel and antiparallel directions could make the perpendicular energy fluxes appear reduced, this is actually not the case, since the perpendicular energy fluxes inside the KSMD are comparable or less than that of the background in Figures 3b–3m. These observations may be understood by the following interpretation. Before the ESWs generation, the energy fluxes have a peak at  $\sim 90^\circ$  pitch angles. Then the parallel and antiparallel electric fields of the ESWs make the electrons difficult to be trapped within the small (ion gyroradius) scale magnetic dip. Therefore the observed

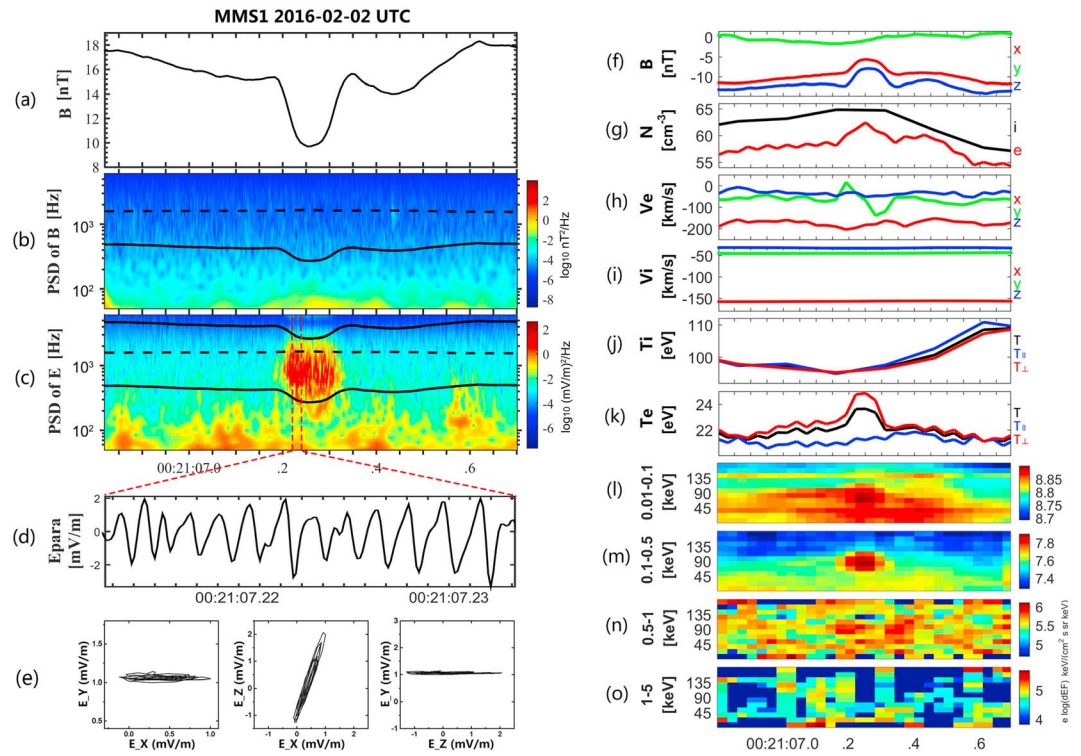


**Figure 4.** Electron cyclotron waves (ECWs) observed in the KSMDs. (a–c) and (f–o) same as Figure 1. The black solid lines in (c) indicate the  $f_{ce}$  and  $3f_{ce}$ . The black dash line is the ion plasma frequency. (d) Parallel electric field. (e) Hodographs of electric field. Plasma properties in (g–k) are calculated by taking the moments from the 3-D particle distributions from 10 eV to 30 keV.

energy flux will increase in parallel and antiparallel directions, and decrease in perpendicular direction when the spacecraft passes through the structure.

Figure 4 shows another kind of electrostatic wave observed by MMS1. The length scale in this case is  $\sim 0.4 \rho_i$ , from  $V \sim 160$  km/s (assuming nonpropagating structure in sheath flow),  $\Delta t \sim 0.15$  s, and  $\rho_i \sim 64$  km from the  $B = 16$  nT and  $E = 105$  eV. The location of the event was  $[6.6, -10.0, -1.2] R_E$ . There is a close correlation between the depression in the magnetic field and the increase of the electric field power spectral densities. These waves populated a frequency range from 0.3 to 1.2 kHz, which corresponds to the range from  $f_{ce}$  to  $3f_{ce}$ . The maximum amplitude of the waves was  $\sim 5$  mV/m and no magnetic field perturbation was observed. The wave mode was linearly polarized, as shown in Figure 4e. These are possibly electrostatic ECWs or EBWs (e.g., Baumjohann & Treumann, 1996; Huang et al., 2016; Tang et al., 2013). The magnetic field strength predominately decreases in  $x$  and  $z$  components (Figure 4f, red and blue lines). An increase in electron number density (Figure 4g, red line) and strong bipolar signature in the  $y$  component of the electron velocity (Figure 4h, green line) were detected. Once again, the ion bulk velocity and temperature do not change significantly across the KSMD (Figures 4i and 4j), but here the  $T_{e\perp}/T_{e\parallel}$  shows a significant increase across the event (Figure 4k). Figures 4l–4n show the electron PADs from MMS1. Electron fluxes near  $90^\circ$  increased both in Figures 4l and 4m. Generally, ECWs are thought to be excited by instabilities due to electron temperature anisotropies or loss cone distributions (e.g., Ashour-Abdalla & Kennel, 1978; Horne & Thorne, 2000; Vaivads et al., 2006). However, loss cone distributions were not observed in the electron PADs in this event. Shown in Figures 4l and 4m, the energy fluxes were asymmetric in parallel and antiparallel directions and significantly enhanced at  $\sim 90^\circ$  pitch angles. This enhancement results in the temperature anisotropy shown in Figure 4k. Therefore, we infer that the ECWs in this case may be driven by the temperature anisotropy.

### 2.3. Statistical Results

A rough statistical analysis is shown in Figure 5. In total, 77 events associated with the three types of waves that we have discussed above are included in this statistics. Twenty-three events are related to the WHs, and

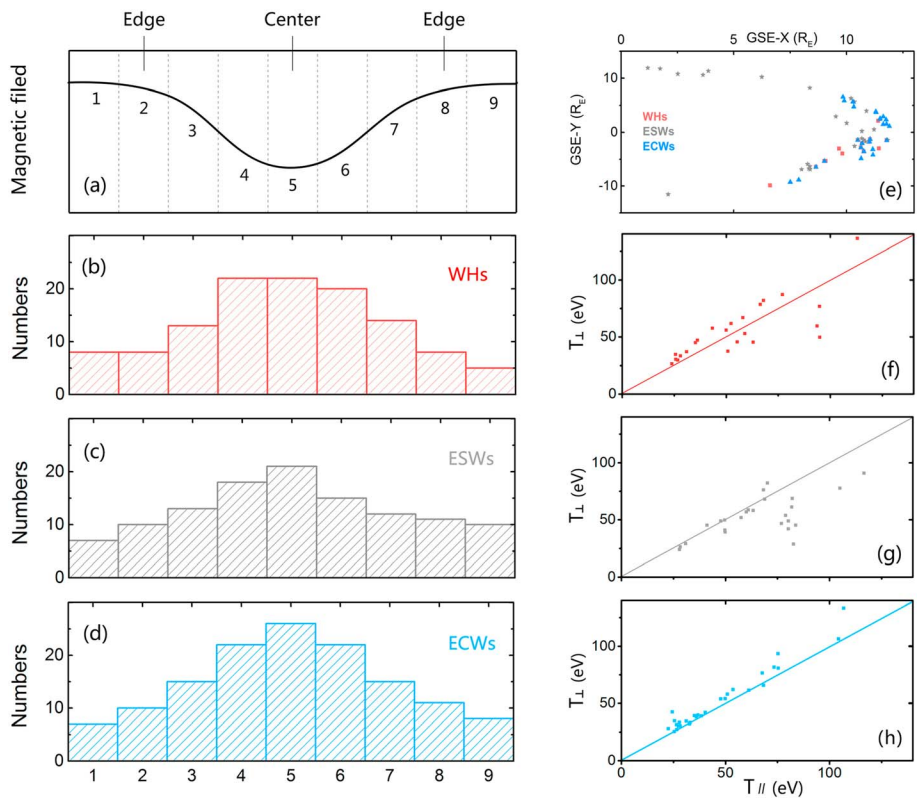


**Figure 5.** Statistical analysis results of the waves. (a) Normalized magnetic dip profile. The numbers indicate the locations with respect to the magnetic dip profile. (b–d) Event numbers versus their locations. (e) Position of the events in geocentric solar ecliptic (GSE) coordinates. (f–h) Electron perpendicular temperature versus parallel temperature of the three types of events. One point represents one event.

25 and 29 events are observed with the ESWs and ECWs, respectively. We investigate the locations within the KSMD where these events are observed. Event locations within the magnetic dip are binned into nine sections as shown in Figure 5a (for more details, please see the supporting information). It can be seen that the occurrence rates for the WHs, ESWs, and ECWs are higher in the center and lower at the edges of KSMD (Figures 5b–5d). If the waves are continuously excited by plasma instabilities inside the KSMDs and propagate from their source, the spacecraft would have more chance to observe the waves in the center of the dip than that at other locations. Thus, we consider that the KSMDs are a possible source for various kinds of waves. More discussions are presented in the next section.

Figure 5e shows the positions of these events in GSE coordinates. Since most of the MMS burst mode data are provided during the magnetopause crossing, the events observed in this study are near the dayside magnetopause (in the magnetosheath). Figures 5f–5h show the perpendicular electron temperature versus the parallel temperature inside the KSMD for each event. In Figure 5f, according to the electron temperature ratio, the statistical results are divided into two classes ( $T_{e\perp} > T_{e\parallel}$  and  $T_{e\parallel} > T_{e\perp}$ ). It is accepted that unstable WHs can be generated by electron temperature anisotropy (e.g., Gary & Karimabadi, 2006; Huang et al., 2012; Huang et al., 2018; Fu et al., 2014) or electron beams (e.g., Feldman et al., 1983; Tokar et al., 1984; Tokar & Gumeft, 1985; Zhang et al., 1999). This suggests that the generation mechanisms could include the electron transverse temperature anisotropy ( $T_{\perp} > T_{\parallel}$ ) and electron beams (more likely to appear as  $T_{\parallel} > T_{\perp}$ , for more details, please see the supporting information). For the ESWs, the temperature anisotropies for the majority of the events (~84%) are less than 1 in Figure 5g. From Figure 3 we know that this is caused by the increase of energy flux in parallel and antiparallel directions. This is consistent with the generation mechanism in previous studies (e.g., Chen et al., 2003; Goldman et al., 1999). On the contrary, for 93% of the ECW events, the temperature anisotropies are greater than 1 in Figure 5h. Hence, one can infer that the generation of the ECWs and the electron temperature anisotropies are linked.

### 3. Discussions

Measurements from in situ field instruments are usually sampled at much higher rates than those from particle instruments. Therefore, the observations of the waves from field instruments provide the highest cadence evidence of kinetic-scale processes within KSMDs. In our study, about one third (77/253) of the events are associated with various kinds of waves. Since these strong wave activities may play important roles in plasma microphysics and may contribute to the energy transfer in space plasma, it is therefore pivotal to understand the relation between the waves and the KSMDs. The statistical results imply that the waves are locally generated in the KSMDs, and thus, the KSMDs could provide a favorable condition for wave generation. For instance, previous studies have shown that electrons with  $\sim 90^\circ$  pitch angle were trapped inside KSMDs in turbulent plasmas and that electron vortices were coupled with KSMDs (e.g., Huang, Sahraoui, et al., 2017; Yao et al., 2017). These lead to higher electron temperature anisotropy inside the structure. The temperature anisotropy may thus provide the free energy required for the excitation and growth of these waves. In previous studies, the existences of KSMDs in turbulent plasmas were studied both by observations and simulations. We therefore consider that the KSMD can transfer energy from turbulent plasmas to the waves.

#### Acknowledgments

The instrumental teams of MMS are greatly appreciated for providing magnetic field, electric field, and plasma data. All the data are available from MMS Science Data Center (<https://lasp.colorado.edu/mms/sdc/public/>). The French involvement (SCM instruments) on MMS is supported by CNES, CNRS-INSIS, and CNRS-INSU. This work was supported by the National Natural Science Foundation of China (grants 41774153, 41574157, 41628402, and 41674165), project supported by the Specialized Research Fund for State Key Laboratories, the International Space Science Institute (ISSI), and the young scholar plan of Shandong University at Weihai (2017WHWLJH08). We appreciate Kaijun Liu for his benefit guidance.

#### References

- Andersson, L., Ergun, R. E., Tao, J., Roux, A., Le Contel, O., Angelopoulos, V., et al. (2009). New features of electron phase space holes observed by the THEMIS mission. *Physical Review Letters*, 102(22), 225004. <https://doi.org/10.1103/PhysRevLett.102.225004>
- Ashour-Abdalla, M., & Kennel, C. F. (1978). Nonconvective and convective electron cyclotron harmonic instabilities. *Journal of Geophysical Research*, 83, 1531–1543. <https://doi.org/10.1029/JA083iA04p01531>
- Bale, S., Kellogg, P. J., Larsen, D. E., Lin, R. P., Goetz, K., & Lepping, R. P. (1998). Bipolar electrostatic structures in the shock transition region: Evidence of electron phase space holes. *Geophysical Research Letters*, 25, 2929–2932. <https://doi.org/10.1029/98GL02111>
- Balikhin, M. A., Sibeck, D. G., Runov, A., & Walker, S. N. (2012). Magnetic holes in the vicinity of dipolarization fronts: Mirror or tearing structures. *Journal of Geophysical Research*, 117, A08229. <https://doi.org/10.1029/2012JA017552>
- Baumjohann, W., & Treumann, R. A. (1996). *Basic space plasma physics* (pp. 275–278). London: Imperial Coll. Press. <https://doi.org/10.1142/p015>
- Burch, J. L., Moore, T. E., Torbert, R. B., & Giles, B. L. (2016). Magnetospheric multiscale overview and science objectives. *Space Science Reviews*, 199(1–4), 5–21. <https://doi.org/10.1007/s11214-015-0164-9>
- Cao, D., Fu, H. S., Cao, J. B., Wang, T. Y., Graham, D. B., Chen, Z. Z., Peng, F. Z., et al. (2017). MMS observations of whistler waves in electron diffusion region. *Geophysical Research Letters*, 44, 3954–3962. <https://doi.org/10.1002/2017GL072703>
- Cattell, C., Dombeck, J., Wygant, J. R., Hudson, M. K., Mozer, F. S., Temerin, M. A., et al. (1999). Comparisons of Polar satellite observations of solitary wave velocities in the plasma sheet boundary and the high altitude cusp to those in the auroral zone. *Geophysical Research Letters*, 26, 425–428. <https://doi.org/10.1029/1998GL900304>
- Chen, L.-J., & Parks, G. K. (2002a). BGK electron solitary waves in 3D magnetized plasma. *Geophysical Research Letters*, 29(9), 1331. <https://doi.org/10.1029/2001GL013385>
- Chen, L.-J., & Parks, G. K. (2002b). BGK electron solitary waves: 1D and 3D. *Nonlinear Processes in Geophysics*, 9(2), 111–119. <https://doi.org/10.5194/npg-9-111-2002>
- Chen, L.-J., Thoule, D. J., & Tang, J.-M. (2003). Width-amplitude relation of Bernstein-Greene-Kruskal solitary waves. <http://arxiv.org/abs/physics/0303021>
- Ergun, R. E., Tucker, S., Westfall, J., Goodrich, K. A., Malaspina, D. M., Summers, D., et al. (2016). The axial double probe and fields signal processing for the MMS Mission. *Space Science Reviews*, 199(1–4), 167–188. <https://doi.org/10.1007/s11214-014-0115-x>
- Feldman, W. C., Anderson, R. C., Bame, S. J., Gary, S. P., Gosling, J. T., McComas, D. J., et al. (1983). Electron velocity distribution near the Earth's bow shock. *Journal of Geophysical Research*, 88, 96–110. <https://doi.org/10.1029/JA088iA01p00096>
- Fu, H. S., Cao, J. B., Cully, C. M., Khotyaintsev, Y. V., Vaivads, A., Angelopoulos, V., et al. (2014). Whistler-mode waves inside flux pileup region: Structured or unstructured? *Journal of Geophysical Research: Space Physics*, 119, 9089–9100. <https://doi.org/10.1002/2014JA020204>
- Fu, H. S., Cao, J. B., Mozer, F. S., Lu, H. Y., & Yang, B. (2012). Chorus intensification in response to interplanetary shock. *Journal of Geophysical Research*, 117, A01203. <https://doi.org/10.1029/2011JA016913>
- Fu, H. S., Cao, J. B., Yang, B., & Lu, H. Y. (2011). Electron loss and acceleration during storm time: The contribution of wave-particle interaction, radial diffusion, and transport processes. *Journal of Geophysical Research*, 116, A10210. <https://doi.org/10.1029/2011JA016672>
- Gary, S. P., & Karimabadi, H. (2006). Linear theory of electron temperature anisotropy instabilities: Whistler, mirror, and Weibel. *Journal of Geophysical Research*, 111, A11224. <https://doi.org/10.1029/2006JA011764>
- Ge, Y. S., McFadden, J. P., Raeder, J., Angelopoulos, V., Larson, D., & Constantinescu, O. D. (2011). Case studies of mirror-mode structures observed by THEMIS in the near-Earth tail during substorms. *Journal of Geophysical Research*, 116, A01209. <https://doi.org/10.1029/2010JA015546>
- Gershman, D. J., Dorelli, J. C., Viñas, A. F., Avanov, L. A., Gliese, U., Barrie, A. C., et al. (2016). Electron dynamics in a subproton-gyroscale magnetic hole. *Geophysical Research Letters*, 43, 4112–4118. <https://doi.org/10.1002/2016GL068545>
- Goldman, M. V., Oppenheim, M. M., & Newman, D. L. (1999). Nonlinear two-stream instabilities as an explanation for auroral bipolar wave structures. *Geophysical Research Letters*, 26, 1821–1824. <https://doi.org/10.1029/1999GL900435>
- Goodrich, K. A., Ergun, R. E., Wilder, F. D., Burch, J., Torbert, R., Khotyaintsev, Y., et al. (2016). MMS multipoint electric field observations of small-scale magnetic holes. *Geophysical Research Letters*, 43, 5953–5959. <https://doi.org/10.1002/2016GL069157>
- Haynes, C. T., Burgess, D., Camporeale, E., & Sundberg, T. (2015). Electron vortex magnetic holes: A nonlinear coherent plasma structure. *Physics of Plasmas*, 22(1), 012309. <https://doi.org/10.1063/1.4906356>

- Horne, R. B., & Thorne, R. M. (2000). Electron pitch angle diffusion by electrostatic electron cyclotron harmonic waves: The origin of pancake distributions. *Journal of Geophysical Research*, 105, 5391–5402. <https://doi.org/10.1029/1999JA900447>
- Huang, S. Y., Du, J. W., Sahraoui, F., Yuan, Z. G., He, J. S., Zhao, J. S., et al. (2017). A statistical study of kinetic-size magnetic holes in turbulent magnetosheath: MMS observations. *Journal of Geophysical Research: Space Physics*, 122, 8577–8588. <https://doi.org/10.1002/2017JA024415>
- Huang, S. Y., Sahraoui, F., Retino, A., Le Contel, O., Yuan, Z. G., Chasapis, A., et al. (2016). MMS observations of ion-scale magnetic island in the magnetosheath turbulent plasma. *Geophysical Research Letters*, 43, 7850–7858. <https://doi.org/10.1002/2016GL070033>
- Huang, S. Y., Sahraoui, F., Yuan, Z. G., He, J. S., Zhao, J. S., Le Contel, O., et al. (2017). Magnetospheric multiscale observations of electron vortex magnetic hole in the magnetosheath turbulent plasma. *Astrophysical Journal*, 836(2). <https://doi.org/10.3847/2041-8213/aa5f50>
- Huang, S. Y., Sahraoui, F., Yuan, Z. G., Le Contel, O., Breuillard, H., He, J. S., et al. (2018). Observations of whistler waves correlated with electron-scale coherent structures in the magnetosheath turbulent plasma. *Astrophysical Journal*, 861(1), 29. <https://doi.org/10.3847/1538-4357/aae831>
- Huang, S. Y., Zhou, M., Deng, X. H., Yuan, Z. G., Pang, Y., Wei, Q., et al. (2012). Kinetic structure and wave properties associated with sharp dipolarization front observed by Cluster. *Annales de Geophysique*, 30(1), 97–107. <https://doi.org/10.5194/angeo-30-97-2012>
- Ji, X.-F., Wang, X.-G., Sun, W.-J., Xiao, C.-J., Shi, Q.-Q., Liu, J., & Pu, Z.-Y. (2014). EMHD theory and observations of electron solitary waves in magnetotail plasmas. *Journal of Geophysical Research: Space Physics*, 119, 4281–4289. <https://doi.org/10.1002/2014JA019924>
- Kennel, C. F., & Engelmann, F. (1966). Velocity space diffusion from weak plasma turbulence in a magnetic field. *Phys. Fluids*, 9(12), 2377–2388. <https://doi.org/10.1063/1.1761629>
- Kojima, H., Matsumoto, H., Chikuba, S., Horiyama, S., Ashour-Abdalla, M., & Anderson, R. R. (1997). GEOTAIL Waveform Observations of broadband/narrowband electrostatic noise in the distant tail. *Journal of Geophysical Research*, 102, 14,439–14,455. <https://doi.org/10.1029/97JA00684>
- Lakhina, G. S., Singh, S. V., Rubia, R., & Sreraj, T. (2018). A review of nonlinear fluid models for ion-and electron-acoustic solitons and double layers: Application to weak double layers and electrostatic solitary waves in the solar wind and the lunar wake. *Physics of Plasmas*, 25(8), 080501. <https://doi.org/10.1063/1.5033498>
- Lakhina, G. S., Tsurutani, B. T., Kojima, H., & Matsumoto, H. (2000). "Broadband" plasma waves in the boundary layers. *Journal of Geophysical Research*, 105, 27,791–27,831. <https://doi.org/10.1029/2000JA009005>
- Le Contel, O., Leroy, P., Roux, A., Coillot, C., Alison, D., Bouabdellah, A., Mirioni, L., et al. (2016). The search-coil magnetometer for MMS. *Space Science Reviews*, 199(1–4), 257–282. <https://doi.org/10.1007/s11214-014-0096-9>
- Le Contel, O., Nakamura, R., Breuillard, H., Argall, M. R., Graham, D. B., Fischer, D., et al. (2017). Lower hybrid drift waves and electromagnetic electron space-phase holes associated with dipolarization fronts and field-aligned currents observed by the Magnetospheric Multiscale mission during a substorm. *Journal of Geophysical Research: Space Physics*, 122, 12,236–12,257. <https://doi.org/10.1002/2017JA024550>
- Li, J., Bortnik, J., An, X., Li, W., Thorne, R. M., Zhou, M., et al. (2017). Chorus wave modulation of Langmuir waves in the radiation belts. *Geophysical Research Letters*, 44, 11,713–11,721. <https://doi.org/10.1002/2017GL075877>
- Li, L., Zhou, X. Z., Zong, Q. G., Chen, X. R., Zou, H., Ren, J., et al. (2017). Ultralow frequency wave characteristics extracted from particle data: Application of IGSO observations. *Science China Technological Sciences*, 60(3), 419–424. <https://doi.org/10.1007/s11431-016-0702-4>
- Li, L., Zhou, X.-Z., Zong, Q.-G., Rankin, R., Zou, H., Liu, Y., et al. (2017). Charged particle behavior in localized ultralow frequency waves: Theory and observations. *Geophysical Research Letters*, 44, 5900–5908. <https://doi.org/10.1002/2017GL073392>
- Li, Z.-Y., Sun, W.-J., Wang, X.-G., Shi, Q.-Q., Xiao, C.-J., Pu, Z.-Y., et al. (2016). An EMHD soliton model for small-scale magnetic holes in magnetospheric plasmas. *Journal of Geophysical Research: Space Physics*, 121, 4180–4190. <https://doi.org/10.1002/2016JA022424>
- Lin, N., Kellogg, P. J., MacDowall, R. J., Tsurutani, B. T., & Ho, C. M. (1996). Langmuir waves associated with discontinuities in the solar wind: A statistical study. *Astronomy and Astrophysics*, 316, 425–429.
- Lindqvist, P.-A., Olsson, G., Torbert, R. B., King, B., Granoff, M., Rau, D., et al. (2016). The spin-plane double probe electric field instrument for MMS. *Space Science Reviews*, 199(1–4), 137–165. <https://doi.org/10.1007/s11214-014-0116-9>
- Mangeney, A., Salem, C., Lacombe, C., Bougeret, J. L., Perche, C., Manning, R., et al. (1999). WIND observations of coherent electrostatic waves in the solar wind. *Annales Geophysicae*, 17, 307–320.
- Matsumoto, H., Deng, X. H., Kojima, H., & Mukai, T. (2000). Correlation between BEN (ESW and NEN) and high-speed plasma flow associated with Reconnection: Geotail observations. *Eos Trans. AGU*, 81(48), Fall meet. Suppl., Abstract SM61A-05.
- Matsumoto, H., Kojima, H., Kasaba, Y., Miyake, T., Anderson, R. R., & Mukai, T. (1997). Plasma waves in the upstream and bow shock regions observed by GEOTAIL. *Advanced Space Research*, 20(4–5), 683–693. [https://doi.org/10.1016/S0273-1177\(97\)00456-0](https://doi.org/10.1016/S0273-1177(97)00456-0)
- Matsumoto, H., Kojima, H., Miyatake, T., Omura, Y., Okada, M., Nagano, I., & Tsutsui, M. (1994). Electrostatic solitary waves (ESW) in the magnetotail: BEN wave forms observed by GEOTAILL. *Geophysical Research Letters*, 21, 2915–2918. <https://doi.org/10.1029/94GL01284>
- Mozer, F., Ergun, R., Temerin, M., Cattell, C., Dombeck, J., & Wygant, J. (1997). New features in time domain electric field structures in the auroral acceleration region. *Physical Review Letters*, 79, 1281–1284. <https://doi.org/10.1103/PhysRevLett.79.1281>
- Muschietti, L., Roth, I., Ergun, R. E., & Carlson, C. W. (1999). Analysis and simulation of BGK electron holes. *Nonlinear Processes in Geophysics*, 6(3/4), 211–219. <https://doi.org/10.5194/npg-6-211-1999>
- Paschmann, G., Fazakerley, A. N., & Schwartz, S. J. (1998). Moments of plasma velocity distributions. In *Analysis methods for multi-spacecraft data* (pp. 125–158). Noordwijk, Netherlands: ISSI SA Publications Division.
- Pollock, C., Moore, T., Jacques, A., Burch, J., Giese, U., Saito, Y., et al. (2016). Fast plasma investigation for magnetospheric multiscale. *Space Science Reviews*, 199(1–4), 331–406. <https://doi.org/10.1007/s11214-016-0245-4>
- Roytershteyn, V., Karimabadi, H., & Roberts, A. (2015). Generation of magnetic holes in fully kinetic simulations of collisionless turbulence. *Philosophical Transactions of the Royal Society A*, 373(20140). <https://doi.org/10.1098/rsta.2014.0151>
- Rubia, R., Singh, S. V., & Lakhina, G. S. (2017). Occurrence of electrostatic solitary waves in the lunar wake. *Journal of Geophysical Research: Space Physics*, 122, 9134–9147. <https://doi.org/10.1002/2017JA023972>
- Russell, C. T., Anderson, B. J., Baumjohann, W., Bromund, K. R., Dearborn, D., Fischer, D., et al. (2016). The magnetospheric multiscale magnetometers. *Space Science Reviews*, 199(1–4), 189–256. <https://doi.org/10.1007/s11214-014-0057-3>
- Russell, C. T., Mellott, M. M., Smith, E. J., & King, J. H. (1983). Multiple spacecraft observations of interplanetary shocks: Four spacecraft determination of shock normals. *Journal of Geophysical Research*, 88, 4739–4748. <https://doi.org/10.1029/JA088A006p04739>
- Santoli'k, O., Parrot, M., & Lefèuvre, F. (2003). Singular value decomposition methods for wave propagation analysis. *Radio Science*, 38(1), 1010. <https://doi.org/10.1029/2000RS002523>

- Shi, Q. Q., Hartinger, M., Angelopoulos, V., Zong, Q. G., Zhou, X. Z., Zhou, X. Y., et al. (2013). THEMIS observations of ULF wave excitation in the nightside plasma sheet during sudden impulse events. *Journal of Geophysical Research: Space Physics*, 118, 284–298. <https://doi.org/10.1029/2012JA017984>
- Shi, Q. Q., Hartinger, M. D., Angelopoulos, V., Tian, A. M., Fu, S. Y., Zong, Q. G., et al. (2014). Solar wind pressure pulse-driven magnetospheric vortices and their global consequences. *Journal of Geophysical Research: Space Physics*, 119, 4274–4280. <https://doi.org/10.1002/2013JA019551>
- Shi, Q. Q., Pu, Z. Y., Soucek, J., Zong, Q. G., Fu, S. Y., Xie, L., et al. (2009). Spatial structures of magnetic depression in the Earth's high-altitude cusp: Cluster multipoint observations. *Journal of Geophysical Research*, 114, A10202. <https://doi.org/10.1029/2009JA014283>
- Smith, E. J., Holtzer, R. E., & Russell, C. T. (1969). Magnetic emissions in the magnetosheath at frequencies near 100 Hz. *Journal of Geophysical Research*, 74, 3027–3036. <https://doi.org/10.1029/JA074i011p03027>
- Smith, E. J., & Tsurutani, B. T. (1976). Magnetosheath lion roars. *Journal of Geophysical Research*, 81, 2261. <https://doi.org/10.1029/JA081i013p02261>
- Sun, W. J., Shi, Q. Q., Fu, S. Y., Pu, Z. Y., Dunlop, M. W., Walsh, A. P., et al. (2012). Cluster and TC-1 observation of magnetic holes in the plasma sheet. *Annales de Geophysique*, 30(3), 583–595. <https://doi.org/10.5194/angeo-30-583-2012>
- Sun, W.-J., Slavin, J. A., Fu, S., Raines, J. M., Sundberg, T., Zong, Q. G., et al. (2015). MESSENGER observations of Alfvénic and compressional waves during Mercury's substorms. *Geophysical Research Letters*, 42, 6189–6198. <https://doi.org/10.1002/2015GL065452>
- Sundberg, T., Burgess, D., & Haynes, C. T. (2015). Properties and origin of subproton-scale magnetic holes in the terrestrial plasma sheet. *Journal of Geophysical Research: Space Physics*, 120, 2600–2615. <https://doi.org/10.1002/2014JA020856>
- Tang, X., Cattell, C., Dombeck, J., Dai, L., Wilson, L. B. III, Breneman, A., & Hupach, A. (2013). THEMIS observations of the magnetopause electron diffusion region: Large amplitude waves and heated electrons. *Geophysical Research Letters*, 40, 2884–2890. <https://doi.org/10.1002/grl.50565>
- Tao, J. B., Ergun, R. E., Andersson, L., Bonnell, J. W., Roux, A., Le Contel, O., et al. (2011). A model of electromagnetic electron phase-space holes and its application. *Journal of Geophysical Research*, 116, A11213. <https://doi.org/10.1029/2010JA016054>
- Thorne, R. M., Horne, R. B., Jordanova, V. K., Bortnik, J., & Glauert, S. A. (2006). Interaction of EMIC waves with thermal plasma and radiation belt particles. In K. Takahashi, et al. (Eds.), *Magnetospheric ULF waves: Synthesis and new directions*. *Geophysical Monograph Series* (Vol. 169, pp. 213–223). Washington, DC: American Geophysical Union. <https://doi.org/10.1029/169GM14>
- Thorne, R. M., Ni, B., Tao, X., Horne, R. B., & Meredith, N. P. (2010). Scattering by chorus waves as the dominant cause of diffuse auroral precipitation. *Nature*, 467(7318), 943–946. <https://doi.org/10.1038/nature09467>
- Tokar, R. L., & Gurnett, D. A. (1985). The propagation and growth of whistler mode waves generated by electron beams in the Earth's bow shock. *Journal of Geophysical Research*, 90, 105–114. <https://doi.org/10.1029/JA090iA01p00105>
- Tokar, R. L., Gurnett, D. A., & Feldman, W. C. (1984). Whistler mode turbulence generated by electron beams in the Earth's bow shock. *Journal of Geophysical Research*, 89, 105. <https://doi.org/10.1029/JA089iA01p00105>
- Torbert, R. B., Russell, C. T., Magnes, W., Ergun, R. E., Lindqvist, P. A., Le Contel, O., et al. (2016). The FIELDS instrument suite on MMS: Scientific objectives, measurements, and data products. *Space Science Reviews*, 199(1–4), 105–135. <https://doi.org/10.1007/s11214-014-0109-8>
- Tsurutani, B. T., Dasgupta, B., Arballo, J. K., Lakhina, G. S., & Pickett, J. S. (2003). Magnetic field turbulence, electron heating, magnetic holes, proton cyclotron waves and the onset of bipolar pulse (electron hole) events: A possible unifying scenario. *Nonlinear Processes in Geophysics*, 10(1/2), 27–35. <https://doi.org/10.5194/npg-10-27-2003>
- Tsurutani, B. T., Dasgupta, B., Galvan, C., Neugebauer, M., Lakhina, G. S., Arballo, J. K., et al. (2002). Phase-steepened Alfvén waves, proton perpendicular energization and creation of magnetic holes and magnetic decreases: The ponderomotive force. *Geophysical Research Letters*, 29(24), 2233. <https://doi.org/10.1029/2002GL015652>
- Tsurutani, B. T., Galvan, C., Arballo, J. K., Winterhalter, D., Sakurai, R., Smith, E. J., et al. (2002). Relationship between discontinuities, magnetic holes, magnetic decreases, and nonlinear Alfvén waves: Ulysses observations over the solar poles. *Geophysical Research Letters*, 29(11), 1528. <https://doi.org/10.1029/2001GL013623>
- Tsurutani, B. T., Guarneri, F. L., Echer, E., Lakhina, G. S., & Verkhoglyadova, O. P. (2009). Magnetic decrease formation from <1 AU to ~5 AU: Corotating interaction region reverse shocks. *Journal of Geophysical Research*, 114, A08105. <https://doi.org/10.1029/2009JA013927>
- Tsurutani, B. T., Ho, C. M., Smith, E. J., Neugebauer, M., Goldstein, B. E., Mok, J. S., et al. (1994). The relationship between interplanetary discontinuities and Alfvén waves: Ulysses observations. *Geophysical Research Letters*, 21, 2267–2270. <https://doi.org/10.1029/94GL02194>
- Tsurutani, B. T., Lakhina, G. S., Pickett, J. S., Guarneri, F. L., Lin, N., & Goldstein, B. E. (2005). Nonlinear Alfvén waves, discontinuities, proton perpendicular acceleration, and magnetic holes/decreases in interplanetary space and the magnetosphere: Intermediate shocks? *Nonlinear Processes in Geophysics*, 12(3), 321–336. <https://doi.org/10.5194/npg-12-321-2005>
- Tsurutani, B. T., Lakhina, G. S., Sen, A., Hellinger, P., Glassmeier, K.-H., & Mannucci, A. J. (2018). A review of Alfvénic turbulence in high-speed solar wind streams: Hints from cometary plasma turbulence. *Journal of Geophysical Research: Space Physics*, 123, 2458–2492. <https://doi.org/10.1002/2017JA024203>
- Tsurutani, B. T., Lakhina, G. S., Verkhoglyadova, O. P., Echer, E., Guarneri, F. L., Narita, Y., & Constantinescu, D. O. (2011). Magnetosheath and heliosheath mirror mode structures, interplanetary magnetic decreases, and linear magnetic decreases: Differences and distinguishing features. *Journal of Geophysical Research*, 116, A02103. <https://doi.org/10.1029/2010JA015913>
- Tsurutani, B. T., Lakhina, G. S., Winterhalter, D., Arballo, J. K., Galvan, C., & Sakurai, R. (1999). Energetic particle cross-field diffusion: Interaction with magnetic decreases (MDs), nonlinear. *Processes Geophys.*, 6(3/4), 235–242. <https://doi.org/10.5194/npg-6-235-1999>
- Tsurutani, B. T., Smith, E., Anderson, R., Ogilvie, K., Scudder, J., Baker, D., & Bame, S. (1982). Lion roars and nonoscillatory drift mirror waves in the magnetosheath. *Journal of Geophysical Research*, 87, 6060–6072. <https://doi.org/10.1029/JA087iA08p06060>
- Vaivads, A., Khotyaintsev, Y., Andre, M., & Treumann, R. A. (2006). Plasma waves near reconnection sites. In J. W. Labelle & R. A. Treumann (Eds.), *Geospace electromagnetic waves and radiation, of Lect. Notes Phys.* (Vol. 687, pp. 251–269). Berlin: Springer Verlag.
- Wilson, L. B. III, Koval, A., Szabo, A., Breneman, A., Cattell, C. A., Goetz, K., et al. (2013). Electromagnetic waves and electron anisotropies downstream of supercritical interplanetary shocks. *Journal of Geophysical Research: Space Physics*, 118, 5–16. <https://doi.org/10.1029/2012JA018167>
- Xiao, T., Shi, Q. Q., Tian, A. M., Sun, W. J., Zhang, H., Shen, X. C., & Du, A. M. (2014). Plasma and magnetic-field characteristics of magnetic decreases in the solar wind at 1 AU: Cluster-C1 observations. *Solar Physics*, 289(8), 3175–3195. <https://doi.org/10.1007/s11207-014-0521-y>
- Xiao, T., Shi, Q. Q., Zhang, T. L., Fu, S. Y., Li, L., Zong, Q. G., et al. (2010). Cluster-C1 observations on the geometrical structure of linear magnetic holes in the solar wind at 1 AU. *Annales de Geophysique*, 28(9), 1695–1702. <https://doi.org/10.5194/angeo-28-1695-2010>

- Yao, S. T., Shi, Q. Q., Guo, R. L., Yao, Z. H., Tian, A. M., Degeling, A. W., et al. (2018). Magnetospheric Multiscale observations of electron scale magnetic peak. *Geophysical Research Letters*, 45, 527–537. <https://doi.org/10.1002/2017GL075711>
- Yao, S. T., Shi, Q. Q., Li, Z. Y., Wang, X. G., Tian, A. M., Sun, W. J., et al. (2016). Propagation of small size magnetic holes in the magnetospheric plasma sheet. *Journal of Geophysical Research: Space Physics*, 121, 5510–5519. <https://doi.org/10.1002/2016JA022741>
- Yao, S. T., Shi, Q. Q., Liu, J., Yao, Z. H., Guo, R. L., Ahmadi, N., et al. (2018). Electron dynamics in magnetosheath mirror mode structures, basically accepted by. *Journal of Geophysical Research: Space Physics*, 123, 5561–5570. <https://doi.org/10.1029/2018JA025607>
- Yao, S. T., Wang, X. G., Shi, Q. Q., Pitkänen, T., Hamrin, M., Yao, Z. H., et al. (2017). Observations of kinetic-size magnetic holes in the magnetosheath. *Journal of Geophysical Research: Space Physics*, 122, 1999–2000. <https://doi.org/10.1002/2016JA023858>
- Zhang, X.-J., Artemyev, A., Angelopoulos, V., & Horne, R. B. (2017). Kinetics of sub-ion scale magnetic holes in the near-Earth plasma sheet. *Journal of Geophysical Research: Space Physics*, 122, 10,304–10,317. <https://doi.org/10.1002/2017JA024197>
- Zhang, X. Y., Zong, Q. G., Wang, Y. F., Zhang, H., Xie, L., Fu, S. Y., et al. (2010). ULF waves excited by negative/positive solar wind dynamic pressure impulses at geosynchronous orbit. *Journal of Geophysical Research*, 115, A10221. <https://doi.org/10.1029/2009JA015016>
- Zhang, Y., Matsumoto, H., & Kojima, H. (1999). Whistler mode waves in the magnetotail. *Journal of Geophysical Research*, 104, 28,633–28,644. <https://doi.org/10.1029/1999JA900301>
- Zhima, Z., Cao, J. B., Fu, H. S., Liu, W. L., Chen, L. J., Dunlop, M., et al. (2015). Whistler mode wave generation at the edges of a magnetic dip. *Journal of Geophysical Research: Space Physics*, 120, 2469–2476. <https://doi.org/10.1002/2014JA020786>
- Zong, Q.-G., Zhou, X. Z., Li, X., Song, P., Fu, S. Y., Baker, D. N., et al. (2007). Ultralow frequency modulation of energetic particles in the dayside magnetosphere. *Geophysical Research Letters*, 34, L12105. <https://doi.org/10.1029/2007GL029915>